

Donnan dialysis for tap-water softening

R. Gueccia^a, A.M.M. Alhadidi^b, A. Cipollina^{a,*}, G. Micale^a

^aDipartimento di Ingegneria, Università di Palermo – Viale delle Scienze Ed.6, 90128 Palermo, Italy, Tel. +39 091 23863788/ +39 333 7521739, emails: andrea.cipollina@unipa.it (A. Cipollina), rosa.gueccia@unipa.it (R. Gueccia), giorgiod.maria.micale@unipa.it (G. Micale)

^bFujifilm Manufacturing Europe B.V., P.O. Box: 90156, 5000 LJ Tilburg, The Netherlands, Tel. +31 (0)13 579 1836/ +31 (0)6 5237 4239, email: abduhsalam.alhadidi@fujifilm.com (A.M.M. Alhadidi)

Received 28 February 2020; Accepted 7 May 2020

ABSTRACT

Hard water significantly decreases the lifetime and efficiency of equipment, which has negative technical and economic consequences. A promising technology for the softening of tap water is based on the Donnan dialysis (DD) process. DD is a separation process by which divalent cations can be removed from tap water using cation-exchange membranes (CEMs) and a concentrated salt solution (receiver). No external driving force is required in DD; ion exchange is only due to a chemical potential gradient across the CEMs. The effect of operating parameters that influence the hardness removal and ion fluxes such as receiver concentration (0.5–2 M) and channel flow rate (0.25–0.35 L min⁻¹) was investigated. Contrary to what expected, it was observed that higher salt concentrations in the receiver did not improve the performance. Therefore, it was chosen 1 M as the optimal concentration for the receiver solution. Moreover, a higher flow-rate leads to higher ion-exchanged flux through the membranes thus higher removal efficiency in the batch configuration. A comprehensive mathematical model, consisting of a distributed parameter model with spatial differential equations and a dynamic part including time-differential equations for batch operations, was developed and validated with original experimental data to provide an effective tool for the design and optimization of DD units. With the model, two household systems were designed and simulated based on typical Dutch and German hard feed waters. Three different operating modes were analyzed and compared in terms of outlet target to create more insight into the potential of DD to become a competitive water softening technology.

Keywords: Electromembrane; Ion exchange; Hardness removal; Ion exchange membranes

1. Introduction

In nature, the type and the concentration of ions in water define the water quality. According to the World Health Organization (WHO) standard, the water become unpalatable when the total dissolved solids (TDS) exceeds 1,000 mg L⁻¹ [1]. Nevertheless, freshwater with a TDS less than 1,000 mg L⁻¹ can be classified as unpalatable due to the presence of unsafe or unwanted ions such as lead, mercury, and/or arsenic. Furthermore, some other

freshwater resources contain a high concentration of divalent ions, mainly calcium and magnesium, which are responsible for the hardness of the water. WHO standard has defined the acceptable limit for water hardness as 120 mg L⁻¹ of CaCO₃ [1]. The limit can be expressed in different units (German hardness degree dGH, French hardness degree dfH, or others).

Despite the controversial opinions concerning the effect of water hardness on human health [2,3], water hardness is a serious proven problem for the drinking water distribution network and industrial and domestic facilities.

* Corresponding author.

In fact, the precipitation of calcium and magnesium sediments caused by the low solubility in water of these salts is the cause of piping clogging and equipment energy usage increase as well as the decrease of their lifetime. Besides, ions promoting the hardness in the water may interact with the surfactants resulting in higher soap consumption [4].

Many applications and research efforts have been spent to supply high-quality water to communities and industries.

Nowadays, the predominant technology for water softening, used for both point-of-entry and point-of-use water treatment, is the cross-linked ion exchange resin (IX-resin), in which the functional groups have the ability to exchange ions from surrounding aqueous solutions.

In the water softener application, cation-exchange resins are used to replace the Ca^{2+} and Mg^{2+} ions with Na^+ ions [5].

The efficiency of such a system is subjected to the saturation of the resin with the divalent cations. Therefore, a regeneration step is required once the resin become saturated and hardness removal is getting below the set threshold. The regeneration step is made using high concentrated NaCl solution. Yearly, the regeneration step results in a significant amount of brine dumped to the sewage system, which may cause a huge disturbance for the wastewater treatment system. On the other hand, IX-resin systems show a low CAPEX and OPEX for low salinity waters (typically below 1 g L^{-1}) [6]. For most of the IX-resin systems, in fact, the energy consumption is very low and it does not require extra pumping cost. Besides that, most IX-resin systems reach a water recovery $> 90\%$ and a lifetime up to 10–15 y [7,8].

A promising branch is related to the electrochemical softening which propose water softening by avoiding the dose of salt and the production of a concentrated brine to be disposed of [9,10], thanks to the pH increase in the proximity of the cathode, which modifies the carbonate equilibrium resulting in the precipitation of CaCO_3 and $\text{Mg}(\text{OH})_2$. However, the high electrode area requirement and the challenging cathode regeneration has limited the applications of electrochemical water softening technology.

Low-pressure reverse osmosis and nanofiltration processes are based on a hydrostatic pressure difference across the membrane as a driving force for the separation and can be used for the softening of surface and groundwater [11]. These systems require high inlet pressure and post pumping systems. The energy consumption of such a system may reach values above 1 kWh m^{-3} in combination with low water recovery. However, the most significant disadvantage of reverse osmosis is the production of a highly concentrated brine to be disposed of.

The ion exchange membrane is widely used for softening applications [12]. An electrical potential is required in the electrodialysis (ED) process [13,14], which generates an organized ions migration from one side to the other of the membrane, resulting in the separation of a dilute and a concentrated stream.

ED-derived technologies, characterized by the type of electrodes, membranes, draw solutions and cell configuration applied, have been widely employed in softening applications such as electrodialysis reversal [15], capacitive deionization [16,17] or electrodeionization [15,18].

Considering the household peak demand of softened water, high electrode capacity and large membrane area are

required typically in combination with high energy demand [19–21], despite their high removal efficiency.

The Donnan dialysis (DD) membrane process is very compelling for its clean nature and operational simplicity, low installation and operating costs, and low energy consumption [22,23].

A key difference between DD and other membrane technologies is that the DD does not employ an electrical potential or pressure across the membrane, no extra energy is required [24]. Rather, the transport of calcium and magnesium ions is promoted by a chemical potential gradient on either side of a cation-exchange membrane (CEM) [25], between the feed (tap-water) and the receiver solution (NaCl solution). It allows ions to be separated continuously.

Up to now, many authors have reported promising results for the removal of Ca^{2+} and Mg^{2+} with DD [22,26,27].

A summary of the available softening technologies is presented in Table 1.

Although the possibility of Donnan applications for water softening has been recognized since long ago, commercial application of this technique is rather limited, and technical information in the literature is scant.

In the present work, a DD module was employed in order to study the effect of process parameters on the divalent cations removal. In addition, a mathematical model able to simulate the process was developed and validated, providing an effective tool for the prediction of all the main process phenomena, and the simulation of real scale continuous or transitory operation.

To study the potential of DD as a competitive water softening technology, three different operation modes of two household systems (designed on typical Dutch and German hard feed waters) were simulated and compared: (I) continuous once-through feed; (II) continuous once-through with feed by-pass; (III) batch operation with product tank. As a result, a commercial system has been proposed.

It is worth noting that the final aim of the present work is to introduce innovative solutions for providing safe and affordable drinking water, the final goal of the EU-funded REvived project.

2. Experimental and modeling approach

2.1. Materials

The solutions for DD experiments were prepared in the laboratory with a concentration of 100 ppm Ca^{2+} and 100 ppm Mg^{2+} , which has a hardness degree of 37.0 dGH. Worth noting that the German hardness (dGH) can be calculated from the sum of the molar concentration of calcium Ca^{2+} and magnesium Mg^{2+} and considering the following equivalence: $1 \text{ dGH} = 0.1783 \text{ mM}$.

In all tests, the receiver solutions consist of NaCl ($M = 58.4 \text{ g mol}^{-1}$) solutions from 0.5 to 2 M.

The membrane adopted is a CEM type 10 from Fujifilm (The Netherlands) and the main characteristics are reported in Table 2.

2.2. DD set-up and experimental procedures

The DD module has a plate and frame configuration, consisting of two endplates equipped with inlet-outlet

Table 1
Comparison of different water softening technologies

Process	Advantages	Disadvantages
Ion-exchange resin	<ul style="list-style-type: none"> • Low running costs • High water recovery • Lifetime up to 10–15 y 	<ul style="list-style-type: none"> • Batch process: frequent regeneration required • Regeneration salt needed • Exchangeable ions in product • Waste receiver requires reclamation or regeneration
Electrochemical process	<ul style="list-style-type: none"> • No salt usage • No brine production 	<ul style="list-style-type: none"> • High specific electrode area requirement • Cathode regeneration
Electrodialysis reversal	<ul style="list-style-type: none"> • Continuous process: no regeneration • High removal efficiency • No salt usage 	<ul style="list-style-type: none"> • Scaling problem • IEMs required • Electrical field required
Electrodeionization	<ul style="list-style-type: none"> • Continuous process: no regeneration • High removal efficiency • No salt usage • Reduced potential drop 	<ul style="list-style-type: none"> • IEMs and IX resins required • Electrical field required • Variable operating conditions
Capacitive deionization	<ul style="list-style-type: none"> • No salt usage • High removal efficiency • Scaling control 	<ul style="list-style-type: none"> • Intermittent process: regeneration step required • Electrical potential required
Reverse osmosis	<ul style="list-style-type: none"> • Membrane life: 5–7 y • Continuous process: no regeneration • No salt usage 	<ul style="list-style-type: none"> • Lower water recovery • Pretreatment of feed water required • High pressures required • Brine production
Donnan dialysis	<ul style="list-style-type: none"> • Low energy consumption: no external driving force required • High water recovery • Simple technology • Continuous process: no regeneration 	<ul style="list-style-type: none"> • Salt usage • Exchangeable ions in product • Low ion fluxes: large IEM surface required • Waste receiver requires reclamation or regeneration

Table 2
Properties of Fujifilm (The Netherlands) type 10 cation-exchange membrane

Item	Specifications
Thickness (dry), μm	125
Electric resistance, $\Omega \text{ cm}^2$	1.59
Permselectivity, %	98.2
Water permeability, $\text{L bar}^{-1} \text{ m}^{-2} \text{ s}^{-1}$	1.5×10^{-6}

manifolds, eleven spacers (thickness 270 μm), and 10 CEMs (active area 10 $\text{cm}^2 \times 10 \text{cm}^2$) interposed between the spacers. Feed and receiver solutions are circulated from/to in the same tanks and they are circulated in a cross-flow direction through the DD module by two magnetic coupled centrifugal pumps (model NH-30PI-Z-D), thus realizing a batch operation mode. The two solutions are continually agitating by using two stirring devices. Fig. 1 schematically illustrates the experimental set-up.

After the module assembly, a leakage test was performed by connecting a volume of water placed on a height

of 2 m (0.2 bar) to one inlet at a time and observing any internal leakage.

Before each experiment, the apparatus was fully fed with a 2 M NaCl solution in order to condition the membrane for 30 min.

Five samples were withdrawn to measure cations concentration variations, the first one after 1 min, the others every 5 min.

All the experiments were performed by using the same volume for the feed and the receiver solutions, equal to 1.5 l. Test with different recovery ratio (ratio between the feed volume and the sum of the feed and receiver volumes) were investigated, and they showed that the removal efficiency decreases with an increase of the recovery, as reported in the supplementary information. However, all the other dependencies were investigated keeping an equal volume of receiver and feed tank, as reported in the following sections.

The repeatability of the DD tests in the lab-scale setup was investigated by repeating a reference experiment for 7 times. From these repeated runs, the 95% confidence interval is calculated and half of its value has been reported as a symmetrical error bar for all experimental points.

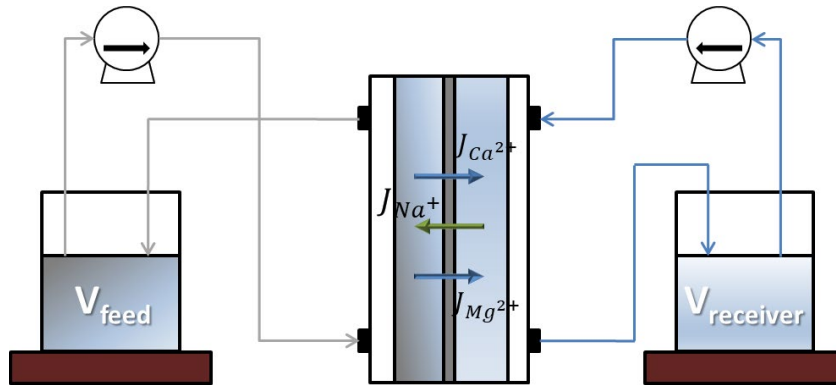


Fig. 1. Experimental set-up adopted for the batch tests at FUJIFILM Manufacturing Europe B.V. Tilburg Laboratories (The Netherlands).

Several operating and performance parameters, such as flux of i -species in solution (J_i) as a function of the test duration and removal efficiency, are calculated from experimental results according to the following equations:

$$J_i = -\frac{\Delta(V^f c_i^f)}{A_m \Delta t} = -\frac{V^f}{A_m} \left(\frac{c_i^f|_{t+\Delta t} - c_i^f|_t}{\Delta t} \right) \quad (1)$$

$$\text{Removal (\%)} = \frac{TH_{\text{init}}^f - TH_{\text{fin}}^f}{TH_{\text{init}}^f} \times 100 \quad (2)$$

where V^f (L) is the feed solution volume; c_i^f (M) is the bulk concentration of the i -component in the feed side; A_m (m²) is the total membrane area and t is the operation time (s).

2.3. Analysis

Density and conductivity for the initial solutions were measured by using an Anton Paar DMA 4500 (Anton-Paar-Straße 20, 8054 Graz, Austria) density meter and a conductivity electrode (WTW ProfiLine Cond 3110 with TetraCon 325/C, Dr.-Karl-Slevogt-Str. 1, 82362, Weilheim, Germany). The concentration of Ca²⁺, Mg²⁺, and Na⁺ cations in the feed and receiver were measured by an inductively coupled plasma optical emission spectrometry (Perkin-Elmer 5300DV ICP-OES, 940 Winter St., Waltham, MA 02451, USA).

2.4. Model for DD

A DD process model based on space and time differential mass balance equations and phenomenological mass transport equations were developed. The model has distributed parameters along the channel length dimension, thus providing information on how concentrations vary along the channel and allowing the simulation of co- and counter-current system configurations. Moreover, time-differential equations simulate the time-variation of concentration in the feed tanks adopted when the system is operated in batch or semi-batch mode.

Despite the modeling of DD systems have been addressed by Davis [28] and simpler Donnan engineering

models are presented in the literature [29–31], the model proposed in the present work aims at providing a comprehensive simulation capability, covering the simulation of time-dependent batch operations or distributed parameters systems in steady-state conditions. Moreover, the model is fully calibrated and validated with real data obtained with novel ion-exchange membranes (IEMs) by FUJIFILM (The Netherlands) and has been used for the design and analysis of either continuous and batch household softener systems (section 3.5) to create more insight into the potential of DD to become a competitive water softening technology.

2.4.1. Spatial differential model equations

DD is a continuous membrane separation process based upon the Donnan equilibrium principle [32]. According to this principle, when electrolyte solutions are placed at opposite sides of a membrane permeable to cations but repulsive to anions and water, the anion composition of the two solutions must remain constant due to the anion rejection of the membrane. However, the cations are under no restraint and will redistribute between the solutions until the equilibrium condition is reached. For each ionic species " i ", the Donnan potentials can be calculated by its respective concentration on each side of the membrane and the concentration inside the membrane itself. Adding these two terms at the two membrane-solution interfaces gives the potential drop available for driving the spontaneous passage of ions through the membrane [Eq. (3)] [33]:

$$E_{\text{Don}} = \frac{RT}{C_{\text{Faraday}}} \ln \left(\frac{a_i^f}{a_i^r} \right)^{\frac{1}{v_i}} \quad (3)$$

where E_{Don} is the Donnan potential (V), R is the gas constant (8.314 J K⁻¹ mol⁻¹), T is the temperature (K), C_{Faraday} is the Faraday constant (96,485 C mol⁻¹), v_i is the valence of the ion ($-$), and a is the activity of ion i (M) in the feed (f) and receiver (r) compartment. This equation is obtained under the assumptions that there is negligible convection through the membrane, electroneutrality is conserved, and the membrane is perfectly permselective (no co-ion transport through the membrane).

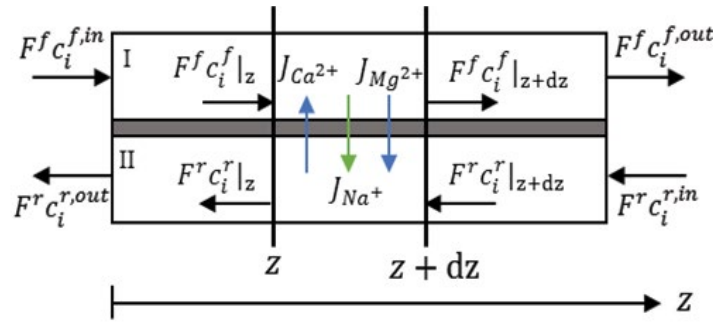


Fig. 2. Schematic representation of the discretized domain of a Donnan dialysis unit, indicating the main fluxes of ions through the membrane and the main involved process variables.

In water softening applications, the divalent cations flux (Mg^{2+} and Ca^{2+}) is coupled with the monovalent sodium flux (Na^+) in order to remove Mg^{2+} and Ca^{2+} cations from the feed solution. The $NaCl$ receiver solution has a much higher concentration as this acts as the main generator of driving force for the transport of Na^+ ions from the receiver into the feed solution. Mg^{2+} and Ca^{2+} ions move in the opposite direction in order to establish the electroneutrality of the system, thus achieving the objective of feed water softening.

Fig. 2 shows the sketch of a counter-current module of length z_{ch} and membrane area A_m indicating the main fluxes of ions through the membrane and suggesting the modeling strategy for the distributed-parameters model described below.

Assuming steady-state conditions and considering diffusive and convective mass transport, the variation of concentration along z -direction in the two channels can be derived from the mass balance on the differential volume between z and $z + dz$:

$$N_i^f = F^f c_i^f \quad (4)$$

$$N_i^f|_z = N_i^f|_{z+dz} + J_i dA_m \quad (5)$$

$$dA_m = dz w_{ch} \quad (6)$$

$$\frac{dN_i^f}{dz} = -J_i w_{ch} \quad (7)$$

$$\frac{dF^f}{dz} = \sum_i \frac{dN_i^f}{dz} \frac{PM_i}{\rho^f} \quad (8)$$

where N_i^f (mol s^{-1}) is the molar flow rate of the i -component in the feed channel; F^f (L s^{-1}) is the volumetric flow rate in the feed channel; J_i ($\text{mol m}^{-2} \text{s}^{-1}$) is the molar flux of the i -component through the membrane; dA_m is the differential membrane area; dz is the differential channel length; w_{ch} (m) is the channel width; PM_i (g mol^{-1}) and ρ^f (g L^{-1}) are molecular weight and density of the feed solution, respectively.

By analogy, same equations for the molar and volumetric flow rates can be derived for the receiver compartment:

$$\frac{dN_i^r}{dz} = J_i w_{ch} \quad (9)$$

$$\frac{dF^r}{dz} = \sum_i \frac{dN_i^r}{dz} \frac{PM_i}{\rho^r} \quad (10)$$

The superscripts f and r indicate feed and receiver, respectively.

The boundary conditions for the two feeds are:

$$z = 0 \quad c_i^f = c_i^{f,in} \quad (11)$$

$$z = z_{ch} \quad c_i^r = c_i^{r,in} \quad (12)$$

The total potential, $E_{Don,tot}$ which is established in such condition, is the sum of the potentials of each species and can be calculated as:

$$E_{Don,tot} = E_{Na^+} + E_{Mg^{2+}} + E_{Ca^{2+}} = \frac{RT}{C_{Faraday}} \ln \left[\left(\frac{c_{Na^+}^r}{c_{Na^+}^f} \right) \left(\frac{c_{Mg^{2+}}^f}{c_{Mg^{2+}}^r} \right)^{0,5} \left(\frac{c_{Ca^{2+}}^f}{c_{Ca^{2+}}^r} \right)^{0,5} \right] \quad (13)$$

The flux of divalent cations across the membrane is proportional to the total potential with a coefficient that can be seen as an apparent “migrative permeability” (though, dimensionally, it is not a permeability) of the membrane to the same cations:

$$J_{Mg^{2+} \& Ca^{2+}} = U \left(c_{Mg^{2+}, Ca^{2+}}^f \right) E_{Don,tot} \quad (14)$$

$$c_{Mg^{2+}, Ca^{2+}}^f = \frac{c_{Mg^{2+}}^f + c_{Ca^{2+}}^f}{2} \quad (15)$$

where $J_{Mg^{2+} \& Ca^{2+}}$ is the flux of the divalent cations ($\text{mol m}^{-2} \text{s}^{-1}$), $U \left(c_{Mg^{2+}, Ca^{2+}}^f \right)$ is the apparent “migrative permeability” ($\text{mol m}^{-2} \text{s}^{-1} \text{V}^{-1}$) expressed as a function of the concentration

of the bivalent cation, and $\overline{c_{Mg^{2+}, Ca^{2+}}^f}$ (M) is the average bivalent cations concentration in the feed solution.

The single fluxes of the different divalent cations species are linked to their molar fraction as follows:

$$J_{Mg^{2+}} = x J_{Mg^{2+} \& Ca^{2+}} = \frac{\text{mol}_{Mg^{2+}}}{\text{mol}_{Mg^{2+} + Ca^{2+}}} J_{Mg^{2+} \& Ca^{2+}} \quad (16)$$

$$J_{Ca^{2+}} = (1-x) J_{Mg^{2+} \& Ca^{2+}} \quad (17)$$

To maintain electroneutrality in both solutions the transport of one mole of divalent cations through the membrane requires the transport of 2 moles of Na^+ ions in the opposite direction [Eq. (18)]. Moreover, since the rejection of the membrane to the anions passage is not complete, a diffusive flux of NaCl salt has to be considered from the stripping to the feed solution [Eq. (19)], due to the large difference in NaCl concentration:

$$J_{Na^+} = 2 J_{Mg^{2+} \& Ca^{2+}} \quad (18)$$

$$J_{NaCl} = U(c_{NaCl}^r)(c_{NaCl}^r - c_{NaCl}^f) \quad (19)$$

where $U(c_{NaCl}^r)$ is the NaCl diffusive permeability through the membrane ($m\ s^{-1}$).

Transport of water through the membrane was also modelled by evaluating the osmotic pressure difference between the two compartments [Eq. (20)].

$$J_{os} = P_{os} RT \sum \alpha_i (c_i^r - c_i^f) \quad (20)$$

where J_{os} ($L\ m^{-2}\ s^{-1}$) is the osmotic flux, P_{os} ($L\ bar\ m^{-2}\ s^{-1}$) is the osmotic permeability of the membrane and α is the van't Hoff factor which is the ratio between the actual concentration of particles produced when the substance is dissolved and the concentration of a substance as calculated from its mass. In particular, here it's assumed that the i -component, which are all ionic compounds, are totally dissociated in

solution and the van't Hoff factor for each component is equal to the number of discrete ions.

2.4.2. Time-dependent model equations

In order to simulate the time-dependent variations of concentrations of the two feed tanks in the batch operation mode (Fig. 3), the model also includes a set of dynamic equations consisting of time-differential mass balances (overall and component mass balance) for each tank [34].

$$\frac{dV^f}{dt} = F_{Dyn}^{f,in} - F_{Dyn}^{f,out} \quad (21)$$

$$\frac{dV^f c_{i,tank}^f}{dt} = F_{Dyn}^{f,in} c_{i,Dyn}^{f,in} - F_{Dyn}^{f,out} c_{i,Dyn}^{f,out} \quad (22)$$

where V^f is the volume of the feed tank; $F_{Dyn}^{f,in}$ and $F_{Dyn}^{f,out}$ represent the inlet/outlet volumetric flow-rates in the feed tank, equal to the outlet/inlet receiver stream in the DD unit, respectively.

In the same way, $c_{i,Dyn}^{f,in}$ and $c_{i,Dyn}^{f,out}$ are the inlet/outlet concentrations in the feed tank, equal to the outlet/inlet concentrations of the feed stream in the DD unit, respectively, while $c_{i,tank}^f$ is the concentration of the i -component in the feed tank.

Volume and concentration variations in the receiver tank are calculated from the closure of mass balance equations:

$$\frac{dV^r}{dt} = -\frac{dV^f}{dt} \quad (23)$$

$$\frac{dV^r c_{i,tank}^r}{dt} = -\frac{dV^f c_{i,tank}^f}{dt} \quad (24)$$

In all cases, perfect mixing is assumed in the tanks, thus:

$$c_{i,Dyn}^{f,out} = c_{i,tank}^f \quad (25)$$

$$c_{i,Dyn}^{r,in} = c_{i,tank}^r \quad (26)$$

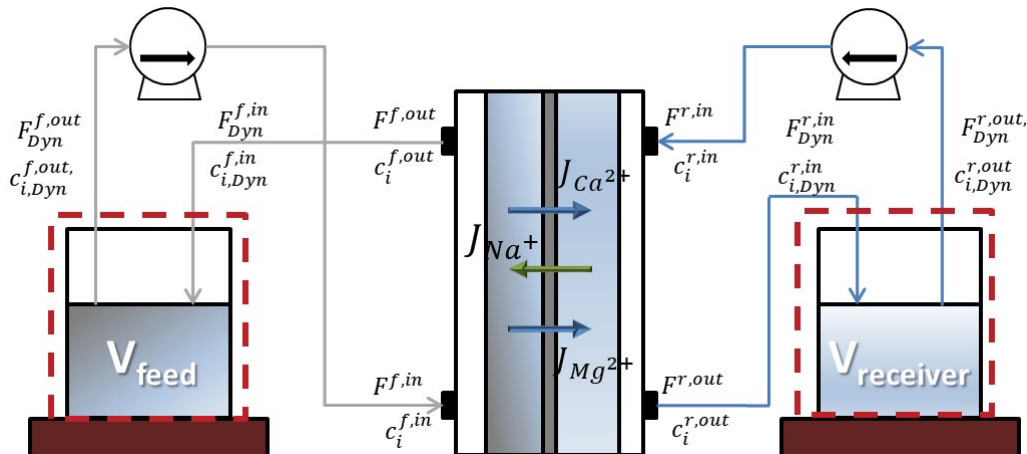


Fig. 3. Schematics of the control volumes in the DD set-up for the dynamic section of the model.

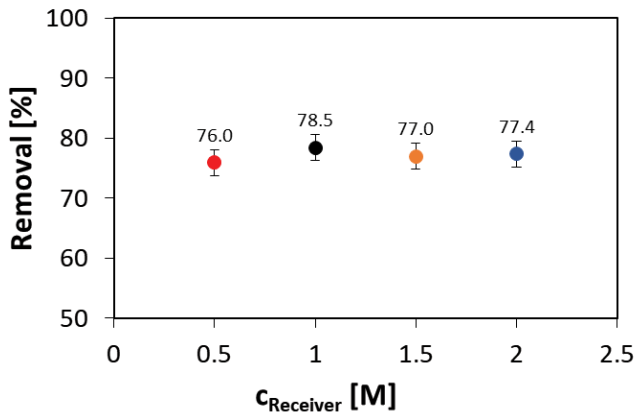


Fig. 4. Ca²⁺ and Mg²⁺ removal vs. receiver concentration. Initial NaCl concentrations in the receiver: 0.5 M (●), 1 M (●), 1.5 M (●), and 2 M (●). Initial Ca²⁺ and Mg²⁺ concentrations in the feed: 100 + 100 ppm.

3. Results and discussion

3.1. Effect of receiver concentration

Several studies on DD have shown that the concentration of the receiver solution is a crucial operation parameter [23,35,36]. In this study, the removal of Mg and Ca cations at different initial receiver concentrations was studied in order to determine removal efficiency. The effect of the receiver concentration on the performance of the DD was examined by testing four different concentrations of NaCl as a receiver solution 0.5, 1, 1.5, and 2 M.

Differently from the literature [26,35], it was observed that the influence of the receiver concentration was not as significant as expected. As shown in Fig. 4, the removal efficiency does not change significantly with the receiver concentration.

3.2. Effect of different flow rate

Another significant operating parameter is the flow rate and, therefore, the linear velocity in the channels, of the two solutions. Two different tests were performed with a flow rate of 0.35 and 0.25 L min⁻¹ and leaving the other operating parameters unchanged. Fig. 5 shows that decreasing

the flow rate through the module channels leads to a lower flux of exchanged ions and, therefore, a lower Ca²⁺ and Mg²⁺ removal. This effect can be attributed to two phenomena: (a) concentration polarization, which is reduced by higher velocities and (b) driving force depletion due to concentration variation along the channel, which is reduced by lower residence times (i.e. higher velocities). Considering that with the adopted linear velocity (over 3 cm s⁻¹) the resistances for convective mass transfer in the boundary layers (polarization phenomena) is normally negligible, the dominant effect remains the lower residence time leading to higher average driving forces in the unit.

3.3. Model calibration and validation

The model was calibrated and, then, validated using original experiments based on laboratory batch tests in a relatively large range of operating conditions (in terms of receiver concentration and flow rates), as reported in section 3.1 and 3.2.

The “migrative permeability” of bivalent cations through the membrane has been correlated to the concentration of the same cations in the feed solution by an accurate model calibration adopting experimental data.

For each experiment, a good fitting between experimental data and model results was obtained by using quadratic correlations for the divalent cations permeability $U(c_{Mg^{2+};Ca^{2+}}^f)$ as a function of the concentration in the feed compartment.

$$U(c_{Mg^{2+};Ca^{2+}}^f) = 33x^2 + 0,23x + 3,57 \cdot 10^{-4} \quad (27)$$

As previously mentioned in section 3.1, a diffusive flux of NaCl salt has to be considered. A linear correlation for the NaCl salt diffusive permeability $P(c_{NaCl}^r)$ was tuned as a correlation of the concentration in the receiver compartment.

$$P(c_{NaCl}^r) = 1,4 \cdot 10^{-8}x - 6 \cdot 10^{-9} \quad (28)$$

It is worth noting that, although the permeability of neutral sodium chloride is quite small in all analyzed conditions, the presence of a significantly high driving force, due to the difference of Na concentration between receiver

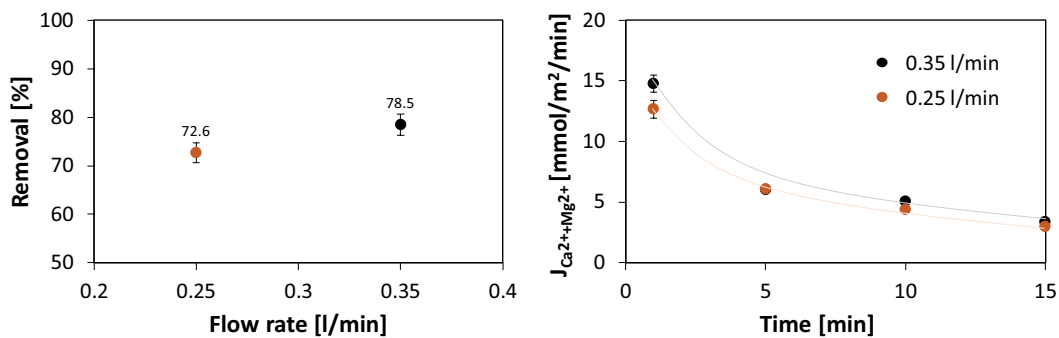


Fig. 5. (a) Ca²⁺ and Mg²⁺ removal vs. flow rate and (b) Ca²⁺ and Mg²⁺ flux vs. time. Flow rate: 0.25 (●) and 0.35 L min⁻¹ (●). Initial NaCl concentrations in the receiver: 1 M. Initial Ca²⁺ and Mg²⁺ concentrations in the feed: 100 + 100 ppm.

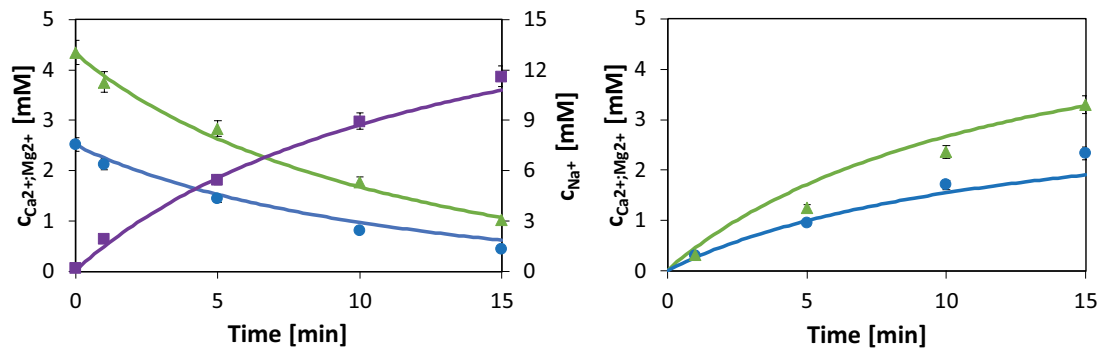


Fig. 6. Comparison between experimental data (Mg^{2+} (\blacktriangle), Ca^{2+} (\bullet) and Na^+ (\blacksquare) solid symbols) and model predictions (continuous line) in the feed (a) and in the receiver (b). Flow rate: 0.35 L min^{-1} . Initial NaCl concentrations in the receiver: 1 M. Initial Ca^{2+} and Mg^{2+} concentrations in the feed: $100 + 100 \text{ ppm}$ ($2.5 + 4.3 \text{ mM}$).

and feed solution, leads to a diffusive flux [Eq. (19)], which may not be negligible compared to the migrative one. This is particularly important in the final part of the channels or at the end of the receiver life cycle when the driving force for Na migrative passage is reduced.

Osmotic water permeability is a membrane characteristic, provided by the manufacturer and already reported in Table 2. However, for the batch test the water flux through the membrane was not considered as the tank volume variations were below 5%, thus considered negligible.

After calibration, the model was validated against several original experimental data.

In Fig. 6, as an example, the time variation of model-predicted and experimental trends of Mg^{2+} , Ca^{2+} , and Na^+ concentration are reported in the feed and receiver tanks for the test with 1 M NaCl receiver.

Such variations can be ascribed to the presence of two opposite fluxes through the membrane: from the feed to receiver channel, as regard the Mg^{2+} and Ca^{2+} cations, and from the receiver to the feed, for the Na^+ cations. In fact, according to the Nernst-Planck equation, which relates the flux to the concentration and potential gradient across the membrane, the cations tend to exchange their position in order to equilibrate the potential.

For the sake of brevity, in Fig. 7, the comparison between experimental data and model predictions is reported in the form of parity plots for all the investigated cases.

A good agreement between model and experiments is observed for all investigated conditions.

3.4. Theoretical analysis of driving forces and performance losses

In order to better understand the DD process behavior and how the operating variables can affect the system performance, the model was adopted to highlight some relevant trends of performance indicators. Among these, the variation of the effective driving force is reported in Fig. 8, considering a semi-batch operation mode (see configuration I in the next paragraph 3.5) with feedwater passing continuously through the unit, while the receiver solution is recirculated in the tank.

In particular, Fig. 8a shows how the total driving force diminishes from the inlet to the outlet of the feed channel

(a part from the curve at time $t = 0$, where the null concentration of Ca^{2+} and Mg^{2+} in the entering receiver solution generates a peak on the right side of the graph) due to the reduction in Ca^{2+} and Mg^{2+} concentration in the feed (or product) solution and the corresponding increase of Na^+ ions in the same, due to the softening process.

However, the two phenomena do not play an equal role. Figs. 8b and c show a separate plot of the two terms of the driving force of Eq. (13), namely the one related to the Na^+ concentration ratio and the second to the $\text{Mg}^{2+} + \text{Ca}^{2+}$ (TH) concentration ratio. It is clear how the effect of sodium concentration decrease in the receiver solution with time does not lead to a significant reduction in the driving force (all curves overlapped), while a significant effect is observed in the reduction of the second term (E_{TH}) of the driving force due to the increase in time of bivalent cations concentration in the receiver solution.

3.5. Configurations for household systems

After validation, the model has been adopted to design and simulate the performance of household systems verifying the feasibility of DD modules for the softening of tap water. With this respect, three different operating modes (Fig. 9) were analyzed and compared in terms of outlet target:

- semi-batch configuration with recycling of receiver solution and a continuous once-through softening of the feedwater;
- semi-batch configuration with the recycling of receiver solution and a by-pass of the feed water designed to regulate the product hardness (by-pass flowrate higher at the beginning, then decreasing to zero over time);
- batch operation with the recycling of receiver solution and a product buffer tank where the softened water is accumulated.

In all cases, the receiver solution is continuously recirculated in the relevant tank.

Worth noting that, the single-pass configuration for the feed and the receiver solutions was excluded a priori because the receiver cannot be continuously wasted. This

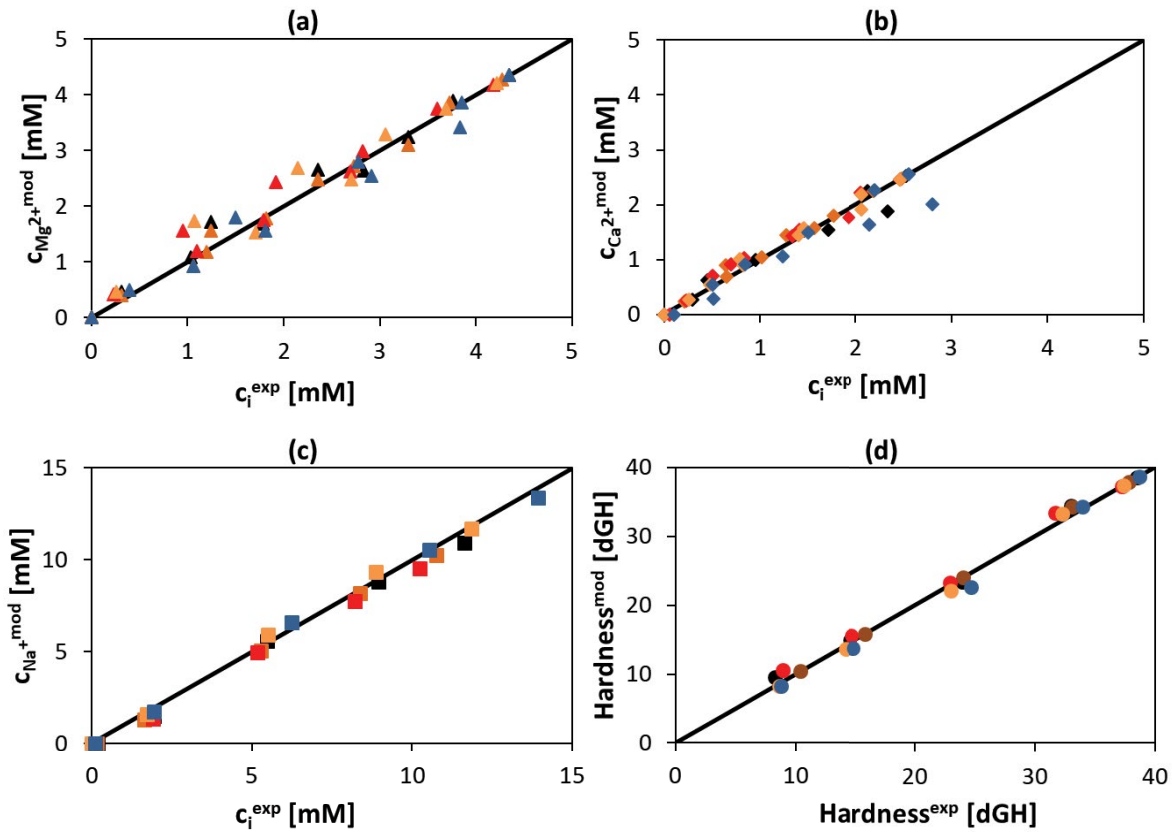


Fig. 7. Parity plots of all experimental (exp) and predicted (mod) values of concentration of Mg^{2+} (a) and Ca^{2+} (b) in feed and receiver tanks, Na^+ (c) in feed tank and total hardness (d) of the softened solution. Tests with NaCl at 0.5 M ($\blacktriangle, \blacklozenge, \blacksquare, \bullet$), 1 M ($\blacktriangle, \blacklozenge, \blacksquare, \bullet$), 1.5 M ($\blacktriangle, \blacklozenge, \blacksquare, \bullet$), 2 M ($\blacktriangle, \blacklozenge, \blacksquare, \bullet$) and 0.35 $L\ min^{-1}$ flow rate; tests with NaCl at 1 M and 0.25 $L\ min^{-1}$ flow rate ($\blacktriangle, \blacklozenge, \blacksquare, \bullet$). Ca^{2+} and Mg^{2+} concentration 100 + 100 ppm (2.5 + 4.3 mM).

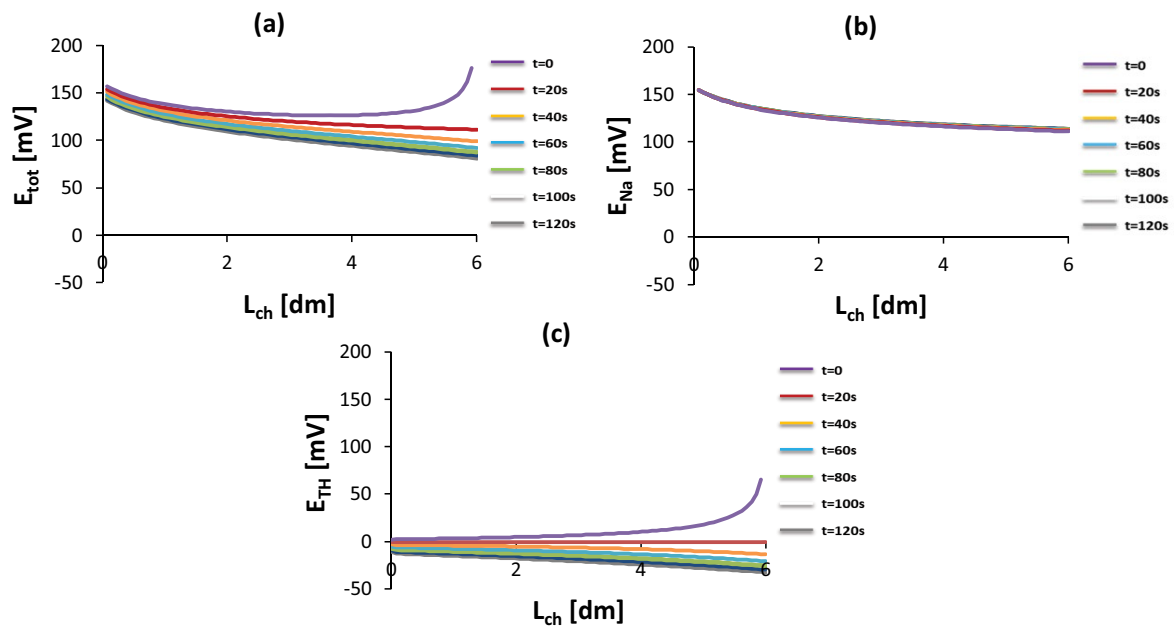


Fig. 8. Variation of the driving force terms (Eq. (13)) through the feed channel and during the time. (a) total driving force, (b) Na^+ concentration driving force term (E_{Na}), and (c) Mg^{2+} and Ca^{2+} concentration driving force term (E_{TH}). Tests with an initial concentration of NaCl 1 M, Mg^{2+} 100 ppm and Ca^{2+} 100 ppm. 10 $L\ min^{-1}$ flow rate and receiver volume 20 L. Total membrane area 8.4 m^2 .

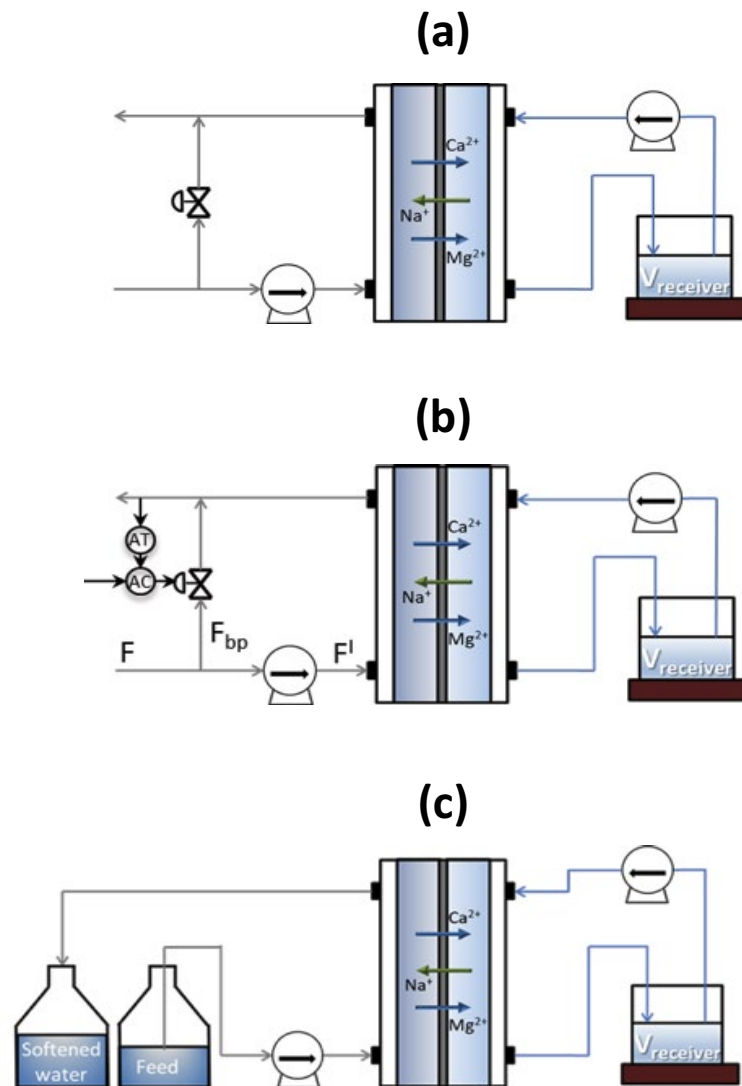


Fig. 9. Schematics of the three-unit configurations (a) continuous once-through feed (I) and (b) continuous once-through with feed by-pass (II); batch operation with product tank (III).

configuration would never be economically advantageous and comparable with other commercial technologies as it concerns salt consumption.

The first step to run the household scenarios simulation was to design the DD module. Reference characteristics of hard water from two different locations in the Netherlands (NL) and in Germany (DE) were considered. The total hardness is around 10 dGH (given by a Ca^{2+} and Mg^{2+} concentration of 60 and 5 ppm, respectively), for the Dutch case, while it is about 2 times higher for the German case with a concentration of Ca^{2+} and Mg^{2+} of 100 and 20 ppm, respectively.

Based on this information, the design strategy has focused on the idea that the module has to guarantee the achievement of the softening target at the end of the life cycle of the receiver solution. For that purpose, the volume and the initial composition of the receiver were fixed at 10 L and 1 M, respectively, while the feed volumes to be

treated were derived by fixing the NaCl consumption per liter of treated water. These values were assumed equal to salt consumption data obtained from a benchmarking investigation performed with two ion exchange resin systems. A summary data obtained from the experimental campaign for the two systems operated in Tilburg (NL) and Frickenhausen (GE) are reported in Table 3.

Thus, fixing the worst condition at which the receiver can operate (namely $[\text{Na}^+] = 0.6 \text{ M}$ and $[\text{Ca}^{2+}] + [\text{Mg}^{2+}] = 0.2 \text{ M}$), a sensitivity analysis has been carried out for the two case studies (Dutch and German water) as presented in Fig. 10.

In particular, the analysis indicates that increasing the membrane area above 0.2 and 0.3 m^2 for the Dutch and German case, respectively, does not lead to significant benefit in terms of product hardness reduction, while it would significantly increase the investment cost of the module. Thus, these membrane areas have been selected for the subsequent simulations.

Table 3
Performance of two IX-resin systems installed in two different locations, Netherlands (NL) and Germany (GE)

	NL	GE
Total product since installation, m ³	313	183
Running days since installation, d	586	514
Running h since installation, h	14,040	12,336
Usage/d, L h ⁻¹	534	256
Regeneration interval, L	698	276
Nr regenerations	449	670
Total salt usage, kg	94	162
Salt usage per regeneration, kg reg ⁻¹	0.21	0.24
Salt consumption, g L ⁻¹	0.3	0.9

Table 4
Household DD module characteristics for the Dutch (NL) and German (DE) case study

Item	NL	DE
Size of membrane (width × length), m	0.2 × 1	0.3 × 1
N° membranes in the DD stack	70	70
Receiver volume, L	10	10
Receiver concentration, M	1	1
Total membrane area, m ²	14	21
Feed flow rate, L min ⁻¹	10	10

Table 5
Salt consumption and volume of treated water for the three different configurations and the two analyzed geographical cases

	I	II	III	case
Salt consumption, g _{NaCl} L _{Hard Water} ⁻¹	0.54	0.45	0.24	NL
	2.47	2.28	1.17	DE
Treated hard water, L	1,080	1,300	2,400	NL
	235	257	500	DE

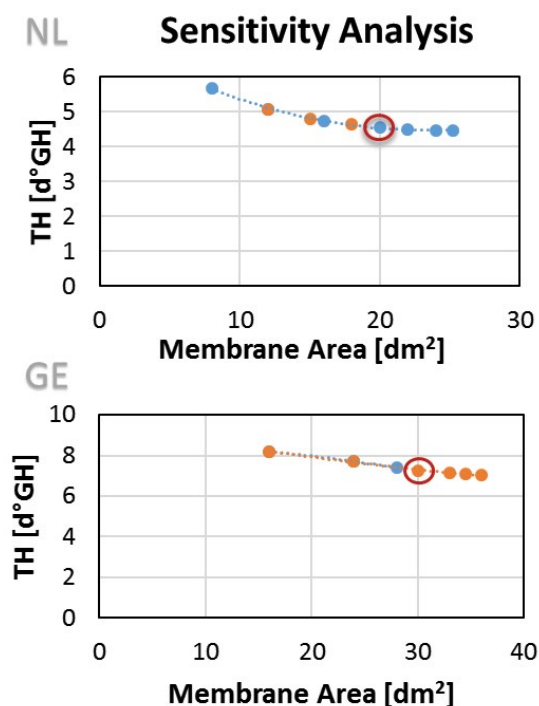


Fig. 10. Dependence of the product water hardness on the DD membrane area for two different typical hard water, Dutch (NL) and German (DE). Membrane width 0.2 (●) and 0.3 m (●).

The detailed characteristics of the DD softening modules so designed are presented in Table 4.

The performance of the three different configurations was compared in terms of total volume of treated water, obtained by multiplying the feed flow rate and the total operation duration, before the hardness of softened water overcomes the threshold limit of 3 dGH.

As shown in Fig. 11 and in Table 5, the feed by-pass integration allows treating a greater amount of hard water and therefore leads to a reduction in salt consumption compared to the semi-batch operation. In fact, continuous softening of the feed water with a by-pass option allows feeding the DD unit with only a portion of the total feed

flow rate, guaranteeing that the product hardness always meets the threshold target fixed, thus enhancing the overall system efficiency.

On the other side, a product buffer tank guarantees an average product hardness lower to the upper threshold for much longer process operation, thus significantly enhancing the system performance in terms of overall softened water volume. In this case, the specific NaCl consumption is consequently reduced, thus improving the process performance even though renouncing to the continuous treatment of the feed water. The Na⁺ concentration decreasing in the receiver is the same for configurations I and III, while it is slightly higher in the configuration II. However, since a total regeneration of the receiver is assumed at the end of the treatment cycle, such a profile has a minor relevance in the present analysis.

For a better understanding, an example of the total driving force trend along the length of the designed DD module for the German case is reported in Fig. 12.

The total driving force at the output of the channel tends to values approaching zero, showing as a further increase of the size of the module would not help the performance of the system.

Looking at the salt consumption per volume unit of softened water in Table 5, the results look quite favorable for the configuration III, which reaches values comparable to the benchmark systems available for the softening of hard water (Table 3). However, moving to the most realistic configurations I and II, the salt consumption increases, reaching values up to 2 times larger than commercial systems.

4. Conclusions

Hard water softening by the DD process was investigated, highlighting the main effects of operating conditions

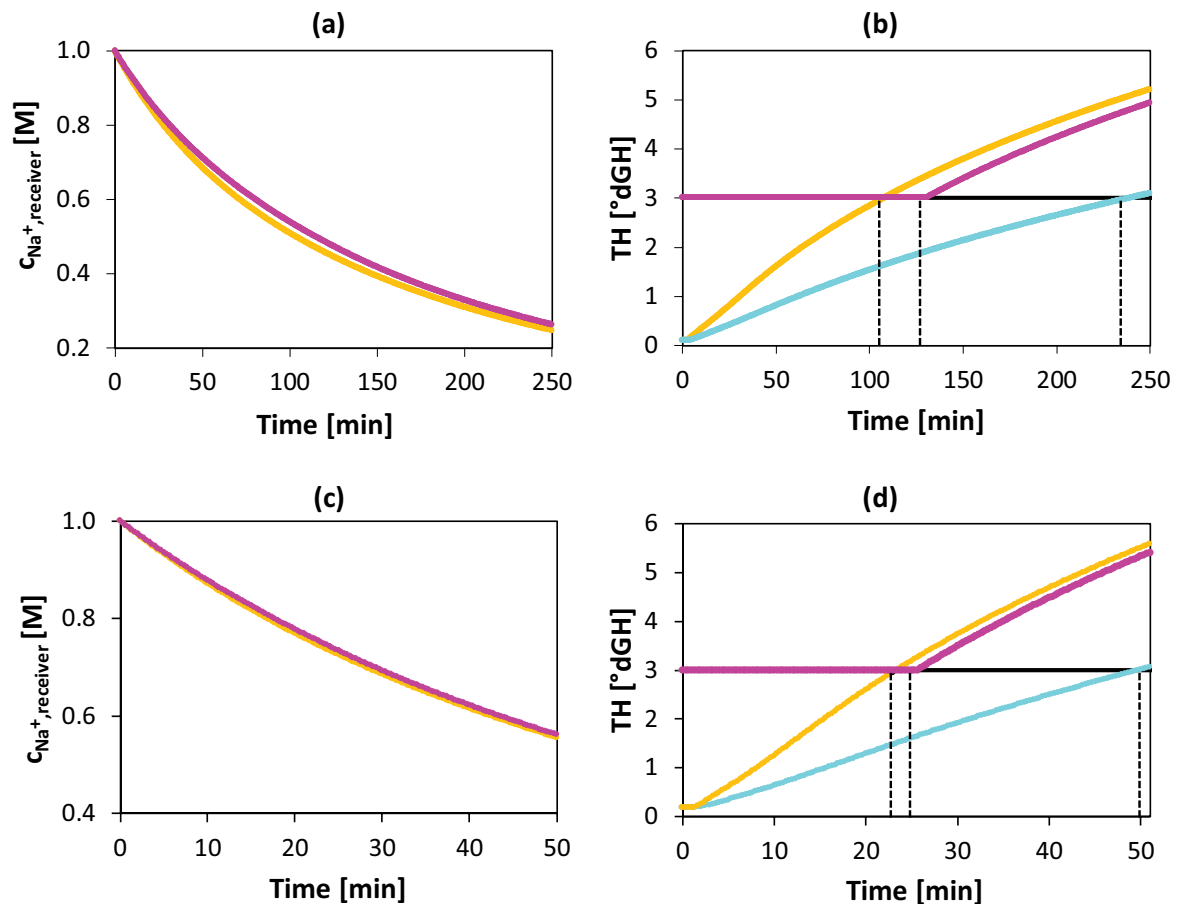


Fig. 11. Model predictions of Na⁺ concentration in the receiver (a and c) and total hardness of softened product water (b and d) vs. time. The configuration I (—), II (—), and III (—). (a and b) NL case; (c and d) DE case.

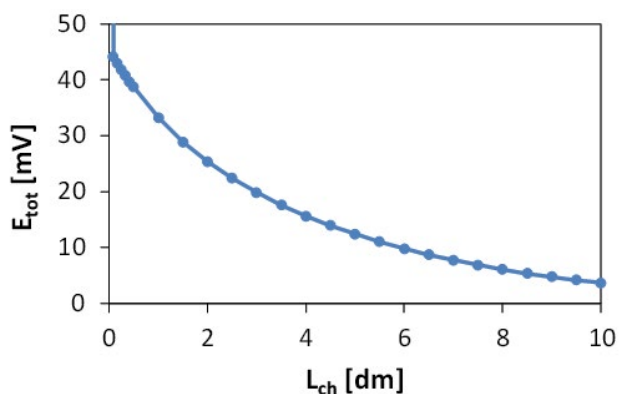


Fig. 12. Variation of the total driving force through the feed channel. Tests with the initial concentration of NaCl 1 M, Mg²⁺ 20 ppm and Ca²⁺ 100 ppm. 10 L min⁻¹ flow rate and receiver volume 10 L. Total membrane area 2 L m².

on process performance. Contrary to what expected, Ca²⁺ and Mg²⁺ ions removal were not significantly enhanced by higher Na⁺ concentration in the receiver because the limiting factor to cations transport from the feed to the stripping solution is the increasing accumulation of Ca²⁺

and Mg²⁺ in the receiver. The effect of flowrate variations on the hardness removal was also investigated, indicating the removal is not enhanced with higher residence time (lower flow rate) if the same volume of receiver and feed solution are considered. However, in all the analyzed cases, removal efficacy is around 75% despite the high initial artificial hard water of 37 dGH.

The whole process was mathematically described within a time/space distributed-parameters model implemented on a spreadsheet with macros and adopted as a process simulator. The model was calibrated and fully validated using the available experimental data in the wide range of NaCl receiver concentrations investigated (0.5–2 M) and for different flow rates of the feed and receiver streams. The model was adopted for the simulation of different household systems of DD operation showing that the proposed technology can be optimized up to being comparable with the commercially available softening systems in terms of salt consumption and volume of treated hard water.

Acknowledgment

This work was financially supported by EU within the REvived water project – Horizon 2020 program, Grant Agreement no. 685579.

Nomenclature and acronyms

CEM	—	Cation exchange membrane
DD	—	Donnan dialysis
dGH	—	Degree german hardness
IEMs	—	Ion exchange membranes
TH	—	Total hardness
A	—	Area, m^2
a	—	Activity, $mol\ L^{-1}$
c	—	Molar concentration, $mol\ L^{-1}$
$C_{Faraday}$	—	Faraday constant, $C\ mol^{-1}$
E	—	Potential, V
F	—	Volumetric flow rate, $L\ s^{-1}$
J	—	Molar flux, $mol\ m^{-2}\ s^{-1}$
N	—	Molar flow rate, $mol\ s^{-1}$
P	—	Diffusive permeability, $m\ s^{-1}$
PM	—	Molecular weight, $g\ mol^{-1}$
P_{os}	—	Osmotic permeability, $L\ bar^{-1}\ m^{-2}\ s^{-1}$
R	—	Gas constant, $L\ bar\ K^{-1}\ mol^{-1}$
T	—	Temperature, K
t	—	Time, s
U	—	Apparent permeability, $mol\ m^{-2}\ s^{-1}\ V^{-1}$
V	—	Volume, L
w	—	Width, m
z	—	Length, m
α	—	Van't Hoff coefficient
ρ	—	Density, $g\ L^{-1}$
v	—	Valence number, —

Subscripts and superscripts

ch	—	Channel
Dyn	—	Dynamic
Don	—	Donnan
exp	—	Experimental
f	—	Feed
fin	—	Final
i	—	Component i , that is, Mg^{2+} , Ca^{2+} , and Na^+
in	—	Inlet
init	—	Initial
m	—	Membrane
mod	—	Modelling
out	—	Outlet
r	—	Receiver
t	—	Time
tank	—	Tank
tot	—	Total

References

- [1] WHO, Acceptability Aspects: Taste, Odour and Appearance, Guidelines for Drinking-Water Quality: Fourth Edition Incorporating the First Addendum, World Health Organization, 20 Avenue Appia, 1211 Geneva 27, Switzerland, 2011, pp. 219–230.
- [2] P. Sengupta, Potential health impacts of hard water, *Int. J. Prev. Med.*, 4 (2013) 866–875.
- [3] D. Tambaru, B.S. Djahi, M.Z. Ndi, The effects of hard water consumption on kidney function: insights from mathematical modelling, *AIP Conf. Proc.*, 1937 (2018) 020020, <https://doi.org/10.1063/1.5026092>.
- [4] K. Gotoh, K. Horibe, Y. Mei, T. Tsujisaka, Effects of water hardness on textile detergency performance in aqueous cleaning systems, *J. Oleo Sci.*, 65 (2016) 123–133.
- [5] P. Sahu, R. Jaiswani, Ion exchange resins: an approach for the development of advanced materials with industrial, pharmaceutical and clinical applications, *Int. J. Adv. Res. Ideas Innovation Technol.*, 4 (2018) 465–481.
- [6] H. Strathmann, Electrodesialysis and its application in the chemical process industry, *Sep. Purif. Rev.*, 14 (1985) 41–66.
- [7] DuPont Ion Exchange Resins Resin Wear-Out Guidelines, Tech Fact, DuPont, 200 Powder Mill Rd., Wilmington, DE 19803, USA, 2019, pp. 1–4.
- [8] W.S. Miller, C.J. Castagna, A.W. Pieper, Understanding Ion-Exchange Resins For Water Treatment Systems, Technical Paper, GE Water & Process Technologies, Daniel-Goldbach-Straße 19, 40880 Ratingen, Germany, 2009, pp. 1–13.
- [9] P. Clauwaert, J. De Paepe, F. Jiang, B. Alonso-Fariñas, E. Vaiooulou, A. Verliefde, K. Rabaey, Electrochemical tap water softening: a zero chemical input approach, *Water Res.* 169 (2020), <https://doi.org/10.1016/j.watres.2019.115263>.
- [10] D. Hasson, V. Lumelsky, G. Greenberg, Y. Pinhas, R. Semiat, Development of the electrochemical scale removal technique for desalination applications, *Desalination*, 230 (2008) 329–342.
- [11] S. Ghizellaoui, A. Chibani, S. Ghizellaoui, Use of nanofiltration for partial softening of very hard water, *Desalination*, 179 (2005) 315–322.
- [12] M. Bodzek, S. Koter, K. Wesołowska, Application of membrane techniques in a water softening process, *Desalination*, 145 (2002) 321–327.
- [13] M. Turek, P. Dydo, Electrodesialysis reversal of calcium sulphate and calcium carbonate supersaturated solution, *Desalination*, 158 (2003) 91–94.
- [14] H. Strathmann, Electrodesialysis, a mature technology with a multitude of new applications, *Desalination*, 264 (2010) 268–288.
- [15] J.-S. Park, J.-H. Song, K.-H. Yeon, S.-H. Moon, Removal of hardness ions from tap water using electromembrane processes, *Desalination*, 202 (2007) 1–8.
- [16] J.M. Choi, P. Dorji, H.K. Shon, S.K. Hong, Applications of capacitive deionization: desalination, softening, selective removal, and energy efficiency, *Desalination*, 449 (2019) 118–130.
- [17] S.-J. Seo, H. Jeon, J.K. Lee, G.-Y. Kim, D.W. Park, H. Nojima, J.Y. Lee, S.-H. Moon, Investigation on removal of hardness ions by capacitive deionization (CDI) for water softening applications, *Water Res.*, 44 (2010) 2267–2275.
- [18] H.-J. Lee, M.-K. Hong, S.-H. Moon, A feasibility study on water softening by electrodeionization with the periodic polarity change, *Desalination*, 284 (2012) 221–227.
- [19] Y.Q. Li, Z.B. Ding, J.F. Li, J.B. Li, T. Lu, L.K. Pan, Highly efficient and stable desalination via novel hybrid capacitive deionization with redox-active polyimide cathode, *Desalination*, 469 (2019) 114098.
- [20] G. Balacco, A. Carbonara, A. Gioia, V. Iacobellis, A.F. Piccinni, Investigation of peak water consumption variability at local scale in Puglia (Southern Italy), *Proceedings*, 2 (2018) 674.
- [21] M. Okamoto, M. Sato, Y. Shodai, M. Kamijo, Identifying the physical properties of showers that influence user satisfaction to aid in developing water-saving showers, *Water (Switzerland)*, 7 (2015) 4054–4062.
- [22] J. Wiśniewski, A. Rózańska, Donnan dialysis for hardness removal from water before electrodesialytic desalination, *Desalination*, 212 (2007) 251–260.
- [23] A. Rózańska, J. Wiśniewski, Modification of brackish water composition by means of Donnan dialysis as pretreatment before desalination, *Desalination*, 240 (2009) 326–332.
- [24] B. Van der Bruggen, Ion-Exchange Membrane Systems—Electrodesialysis and Other Electromembrane Processes, P. Luis, Ed., *Fundamental Modeling of Membrane Systems: Membrane and Process Performance*, 2018, pp. 251–300.
- [25] A. Philippe, A. Vrij, The Donnan equilibrium: I. on the thermodynamic foundation of the Donnan equation of state, *J. Phys. Condens. Matter*, 23 (2011) 194106.
- [26] J. Wiśniewski, A. Rózańska, T. Winnicki, Removal of troublesome anions from water by means of Donnan dialysis, *Desalination*, 182 (2005) 339–346.
- [27] M. Şahin, H. Görçay, E. Kır, Y. Şahin, Removal of calcium and magnesium using polyaniline and derivatives modified

- PVDF cation-exchange membranes by Donnan dialysis, *React. Funct. Polym.*, 69 (2009) 673–680.
- [28] T.A. Davis, *Membrane Processes: Donnan Dialysis, Desalination and Water Resources (DESWARE)*, Encyclopedia of Desalination and Water Resources (DESWARE), 5 Davis Farm Road, Annandale, NJ 08801 USA, 2012.
- [29] S. Ring, D. Hasson, H. Shemer, R. Semiat, Simple modeling of Donnan separation processes, *J. Membr. Sci.*, 476 (2015) 348–355.
- [30] D. Hasson, S. Ring, R. Semiat, H. Shemer, Simple modeling of Donnan separation processes: single and multicomponent feed solutions, *Sep. Sci. Technol.*, 55 (2020) 1216–1226.
- [31] D. Hasson, A. Beck, F. Fingerman, C. Tachman, H. Shemer, R. Semiat, Simple model for characterizing a Donnan dialysis process, *Ind. Eng. Chem. Res.*, 53 (2014) 6094–6102.
- [32] F.G. Donnan, The theory of membrane equilibria, *Chem. Rev.*, 1 (1924) 73–90.
- [33] T. Ktari, C. Larchet, B. Auclair, Mass transfer characterization in Donnan dialysis, *J. Membr. Sci.*, 84 (1993) 53–60.
- [34] R. Gueccia, S. Randazzo, D. Chillura Martino, A. Cipollina, G. Micale, Experimental investigation and modeling of diffusion dialysis for HCl recovery from waste pickling solution, *J. Environ. Manage.*, 235 (2019) 202–212.
- [35] S. Ben Hamouda, K. Touati, M. Ben Amor, Donnan dialysis as membrane process for nitrate removal from drinking water: membrane structure effect, *Arabian J. Chem.*, 10 (2017) S287–S292.
- [36] J. Wiśniewski, A. Różańska, Donnan dialysis with anion-exchange membranes as a pretreatment step before electrodialectic desalination, *Desalination*, 191 (2006) 210–218.

Supplementary information

Several different operating conditions with different recovery ratios (ratio between the feed volume and the sum of the feed and receiver volumes) were investigated, and they showed that the removal efficiency decreases with an increase of the recovery, as shown in Fig. S1. However, since batch results are not representative of real operating conditions (which are reported as an example in section 3.5), these data are not reported in the main article, while all laboratory tests performed for the model calibration/validation have been characterized by a recovery of 50% (an equal volume of feed and receiver), as the reference and simple case.

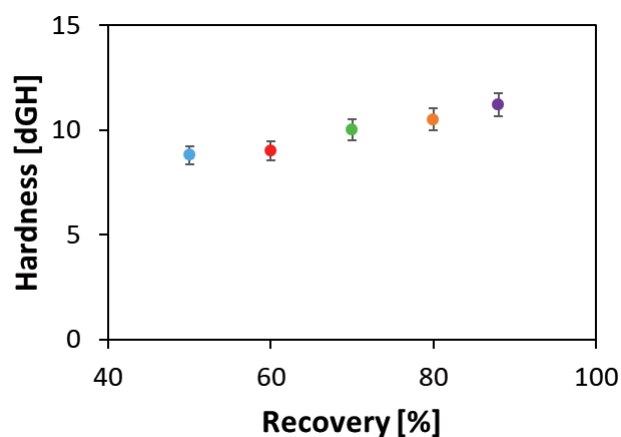


Fig. S1. Total hardness vs. recovery. Feed volume 1.5 L. Receiver volume: 1.5 L (●), 1 L (●), 0.65 L (●), 0.375 L (●) and 0.2 L (●).